Electronic Supplementary Material (ESI) for Nanoscale.

The Role of Interface on the Toughening and Failure Mechanisms of Thermoplastic Nanocomposites Reinforced with Nanofibrillated Rubber

Mahdi Zeidi[a], Chun Il Kim[b*], Chul B Park[a*]

[a] Microcellular Plastics Manufacturing Laboratory, Department of Mechanical and Industrial Engineering, University of Toronto, 5 King's College Road, Toronto, ON, Canada, M5S 3G8.

[b] Department of Mechanical Engineering, University of Alberta, 9211 116 Street NW, Edmonton, AB, Canada, T6G 1H9.

*** Corresponding authors.**

E-mail addresses: m.zeidi@mail.utoronto.ca (Mahdi Zeidi), cikim@ualberta.ca (Chun Il Kim), park@mie.utoronto.ca (Chul B. Park)

Supplementary Information contents:
Number of pages: 9
Number of figures: 5
Number of tables: 4

- **Leonard-Jones Potential Parameters:**

Table S1 Leonard-Jones Potential Parameters.

Pair	σ	ε
c2,c2	0.11800	3.90500
c3,c3	0.16000	3.91000
c32,c32	0.16000	3.91000
c7,c7	0.10500	3.75000
c8,c8	0.11500	3.80000
ch,ch	0.08000	3.85000

- **Force field parameters obtained from the quantum mechanics (QM) simulation:**

The bond and angle force field parameters were obtained by changing the atom separation distance and angle by a magnitude of 0.05 Å and 5°. All energy calculations were carried out by employing complete-active-space second-order perturbation theory (CASPT2/cc-pVTZ)[1].

Table S2 Morse force field parameters (bonds).

Bond	D (Kcal/mol)	r_0(Å)	α	β
c2,c2	95.11	1.526	1.87	0.008
c2,c32	85.65	1.526	1.51	0.078
c2,c7	115.12	1.500	1.33	0.004
c2,ch	65.98	1.526	1.29	0.009
c3,ch	74.32	1.526	1.97	0.075
c32,c8	105.75	1.500	2.11	0.050
c7,c8	121.09	1.340	2.05	0.039
c7,ch	88.72	1.500	1.18	0.024
ch,ch	59.31	1.526	1.54	0.064

Table S3 Anharmonic force field parameters (angles).

Angle	θ_0 (degree)	k_1 (Kcal/mol/rad)	k_2 (Kcal/mol/rad^2)	k_3 (Kcal/mol/rad^3)	k_4 (Kcal/mol/rad^4)
c2,c2,c2	112.400	0.00	43.65	-51.23	0.01
c2,c2,c32	112.400	0.001	89.09	-12.98	0.01
c2,c2,ch	112.400	0.00	77.31	-29.00	0.00
c2,c7,c8	112.700	0.00	69.12	-39.10	0.00
c2,c7,ch	112.700	0.00	89.45	-33.22	0.02
c2,ch,c2	112.400	0.00	61.75	-42.41	0.00
c2,ch,c3	112.400	0.00	-51.32	-74.89	189.83
c2,ch,c7	112.700	0.001	88.53	-11.92	0.00
c2,ch,ch	111.500	0.00	51.82	-50.36	0.00
c3,ch,c3	111.500	0.00	56.38	-28.77	0.00
c3,ch,ch	111.500	0.002	68.99	-20.08	0.04
c32,c2,ch	112.400	0.00	81.11	-15.22	0.00
c32,c8,c7	112.700	0.00	42.32	-31.32	0.00
c7,c2,ch	112.700	0.00	-32.10	-59.43	211.75
c7,ch,ch	112.700	0.00	49.96	-14.13	0.00
c8,c7,ch	112.700	0.001	63.52	-21.11	0.00
ch,c2,ch	112.400	0.00	77.57	-18.12	0.01
ch,ch,ch	111.500	0.00	-39.91	-61.64	108.14

- **Simulation protocol of the EPDM nanofiber formation:**

In Table S3, the detailed description of the four-step MD simulation protocol of the crosslinked-annealed-melt-drawn EPDM nanofiber formation is presented.

Table S4 Nanofiber formation four-step Methodology

Step 1: Bulk-state equilibrium and energy minimization			
Ensemble	Temperature (K)	Duration (ns)	Pressure (bar)
NEV/limit		1	
NPT	150	4	0
NPT	150 to 1000	4	0
NPT	1000 to 800	4	0
NPT	800	4	0 to 1013.25 in all-directions
NPT	800	4	1013.25 to 0 in all-directions
NPT	800 to 150	10	0
NPT	150 to 800	10	0
NPT	800 to 150	4	0
Step 2: Free-surface formation			
NVT	150 to 800	4	
NPT	800	10	0 in z-direction
NPT	800 to 150	4	0 in z-direction
NPT	150	4	0 in z-direction
Step 3: Melt-drawing and employing cylindrical confinement			
NPT	150 to 800	4	0 in z-direction
A linear increased force is applied in the z-direction and the system is confined.			
NPT	800 to 800	4	0 in z-direction
NVT	800 to 150	4	
NPT	150	4	0 in z-direction
Step 4: Crosslinking and Annealing			
NPT	150 to 800	4	0 in z-direction
Reactive simulation is performed for crosslinking (50ns)			
NVT	800 to 150	4	
NPT	150	4	0 in z-direction
The generated nanofiber is then embedded inside the PP matrix and the pull-out and tensile tests are performed.			

- **Nanostructure characterization of EPDM at the bulk-state:**

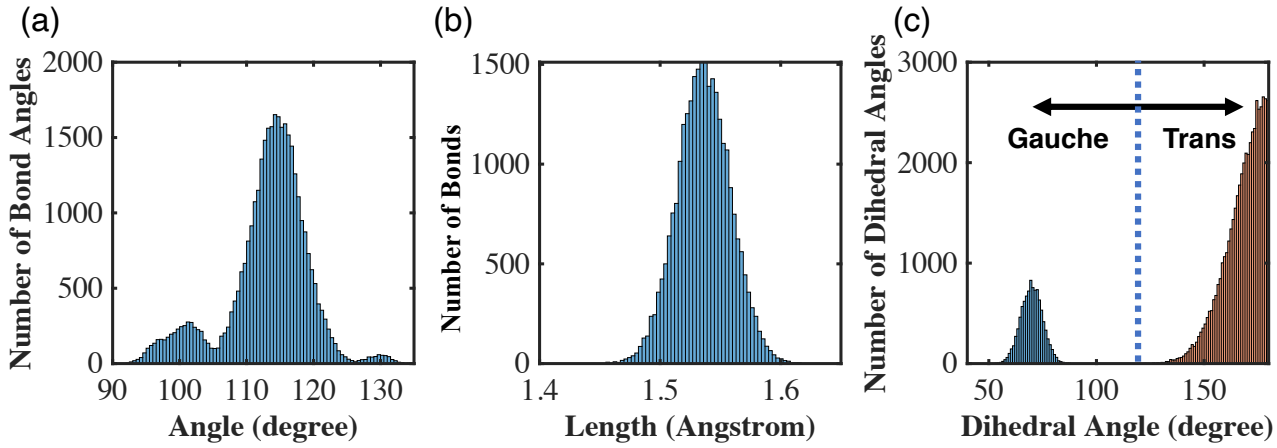

Figure S1 The (a) bond length, (b) bond angle, and (c) dihedral angle distributions for the EPDM at bulk-state after equilibrating the system at 150K.

- **Effect of the melt-drawing process on the polymeric chain orientation:**

The results presented in this section reveal the structural revolution and corresponding abrupt change in mechanical properties (i.e., size dependency) of nanofibers prepared with melt drawing via applied axial force. To investigate the effect of the axial force, two kinds of nanofibers were prepared: with and without applying the axial force (see, Section 2 in paper). In Figure S2a, the effect of axial force on the radius of gyration of one single EPDM polymeric chain was illustrated. As expected, the chain tends to re-orient and align in the direction of axial force (z-axis). In Figure S2b, representative snapshots of the final atomic structures of EPDM nanofibers at different drawing ratios were illustrated. The drawing ratio can be controlled by whether the axial force magnitude or the simulation time. In Figure S2c, comparative snapshots of EPDM nanofibers prepared by both methods are displayed: Figure S2a-left: without axial force and Figure S2a-right: with axial force. Without applying the axial force, polymeric chains are randomly orientated and distributed in the system and the nanofiber is in an amorphous state. However, by applying the axial force (melt-drawing), it was observed that the EPDM chains are well-ordered along the nanofiber's axis. In Figure S2e, the chain orientation parameter (P_{2z}) was monitored at different drawing ratio nanofiber (see Figure S2d for P_{2z} equation). As the drawing ratio increases, the polymeric chains show a tendency to realign in the z-direction. The changes in mechanical properties were also demonstrated in Figs. S3 and S4.

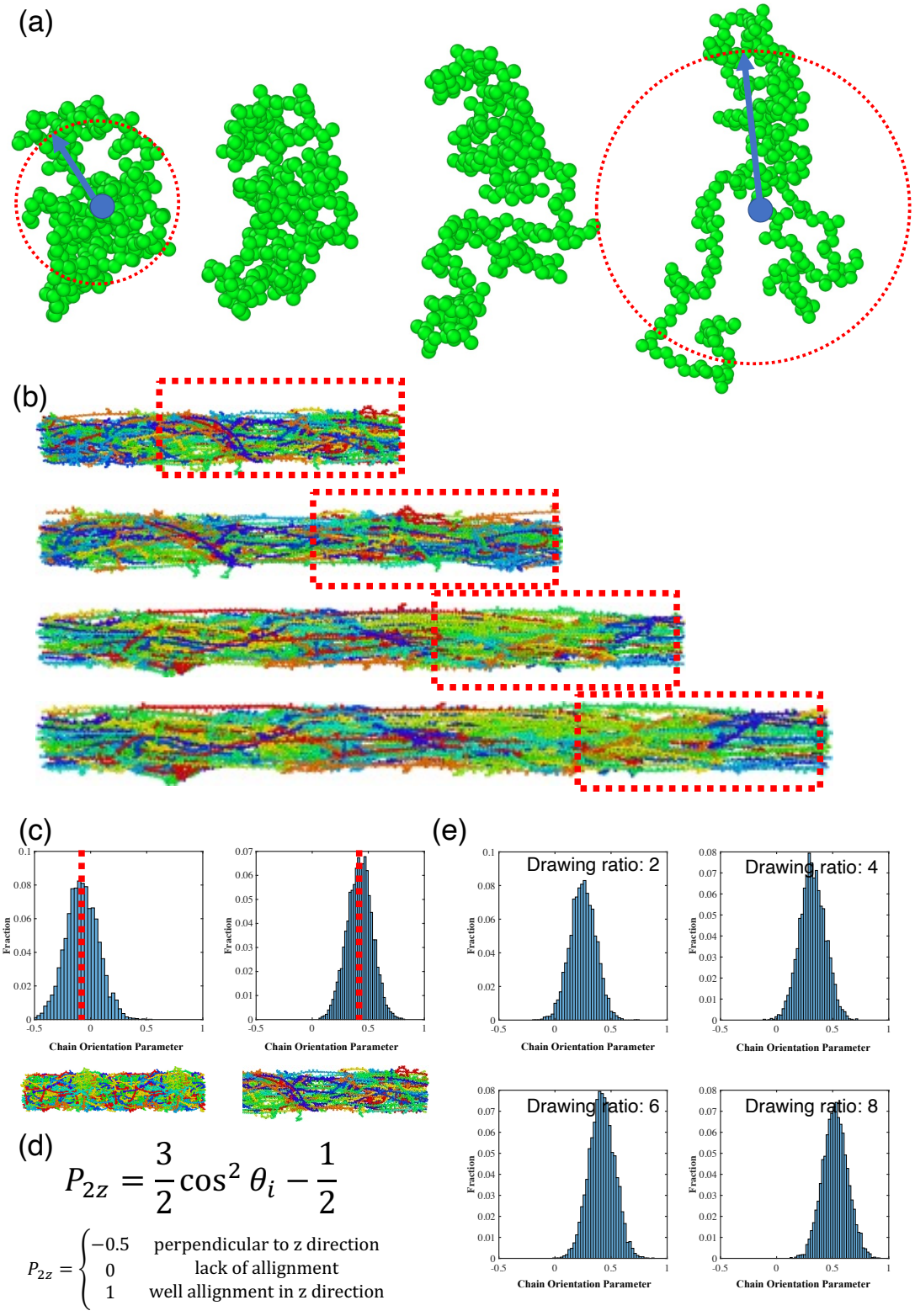

$$P_{2z} = \frac{3}{2}\cos^2\theta_i - \frac{1}{2}$$

$$P_{2z} = \begin{cases} -0.5 & \text{perpendicular to z direction} \\ 0 & \text{lack of allignment} \\ 1 & \text{well allignment in z direction} \end{cases}$$

Figure S2 (a) Snapshot of an individual EPDM chain for various strain, the chains were realigned in the direction of applied load, (b) snapshot of the generated EPDM nanofiber at different drawing ratio, (c) the distribution of the chain orientation parameter (P_{2z}) and representative snapshots of the EPDM nanofibers with and without melt-drawing, (d) the relation of the chain orientation parameter (P_{2z}) of nanofiber: $P_{2z} = -0.5$, $P_{2z} = 0$ and $P_{2z} = 1$ refer to perpendicular to the z-direction, no significant alignment and well-alignment in the z-direction, respectively[2,3], and (e) monitoring of the chain orientation parameter of the nanofibers at different drawing ratios. As the drawing ratio increases, the polymeric chains tend to realign in the z-direction.

- **Effect of the molecular weight on the mechanical properties of the EPDM nanofiber:**

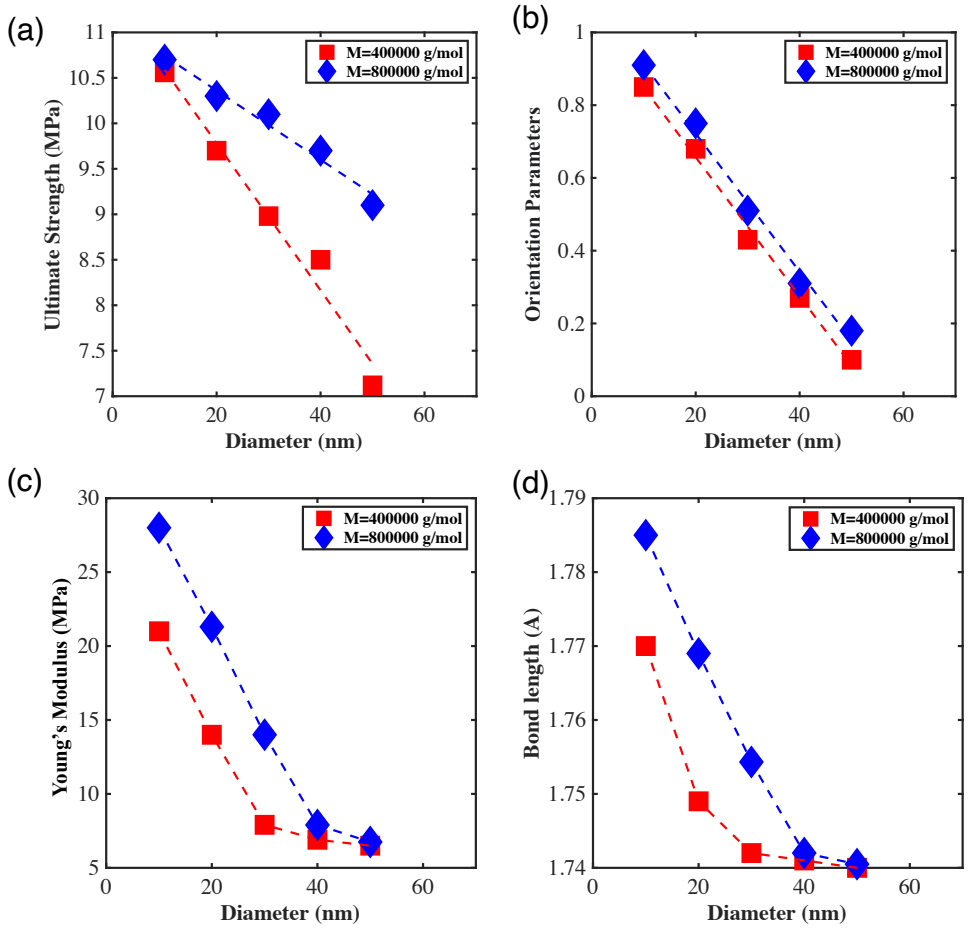

Figure S3 Correlation of (a) EPDM nanofiber diameter vs ultimate tensile strength for different molecular weight (MW) (MW = 400000 g/mol and MW = 800000 g/mol), (b) corresponding nanofiber diameter vs chain orientation parameter, (c) corresponding nanofiber diameter vs. Young's modulus, and (d) corresponding diameter vs. the average length of bonds along the EPDM backbone.

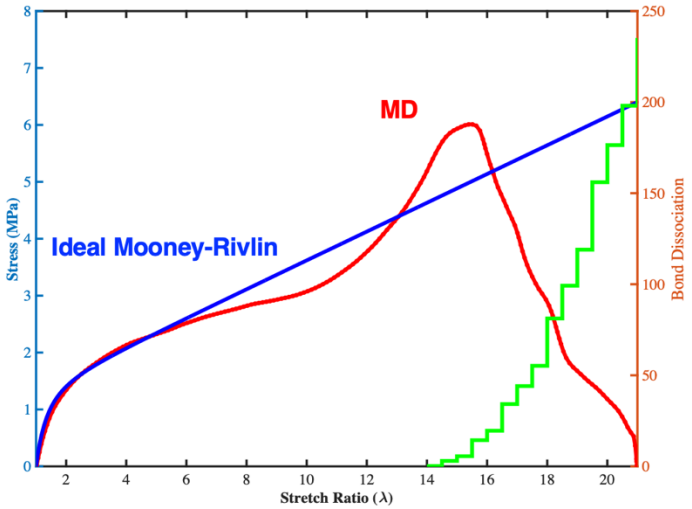

Figure S4 Mechanical behaviour of EPDM nanofiber and the number of covalent bond dissociations calculated from MD simulation.

- **Comparison between mechanical properties and evolution of the potential energies of the annealed and amorphous nanofibers:**

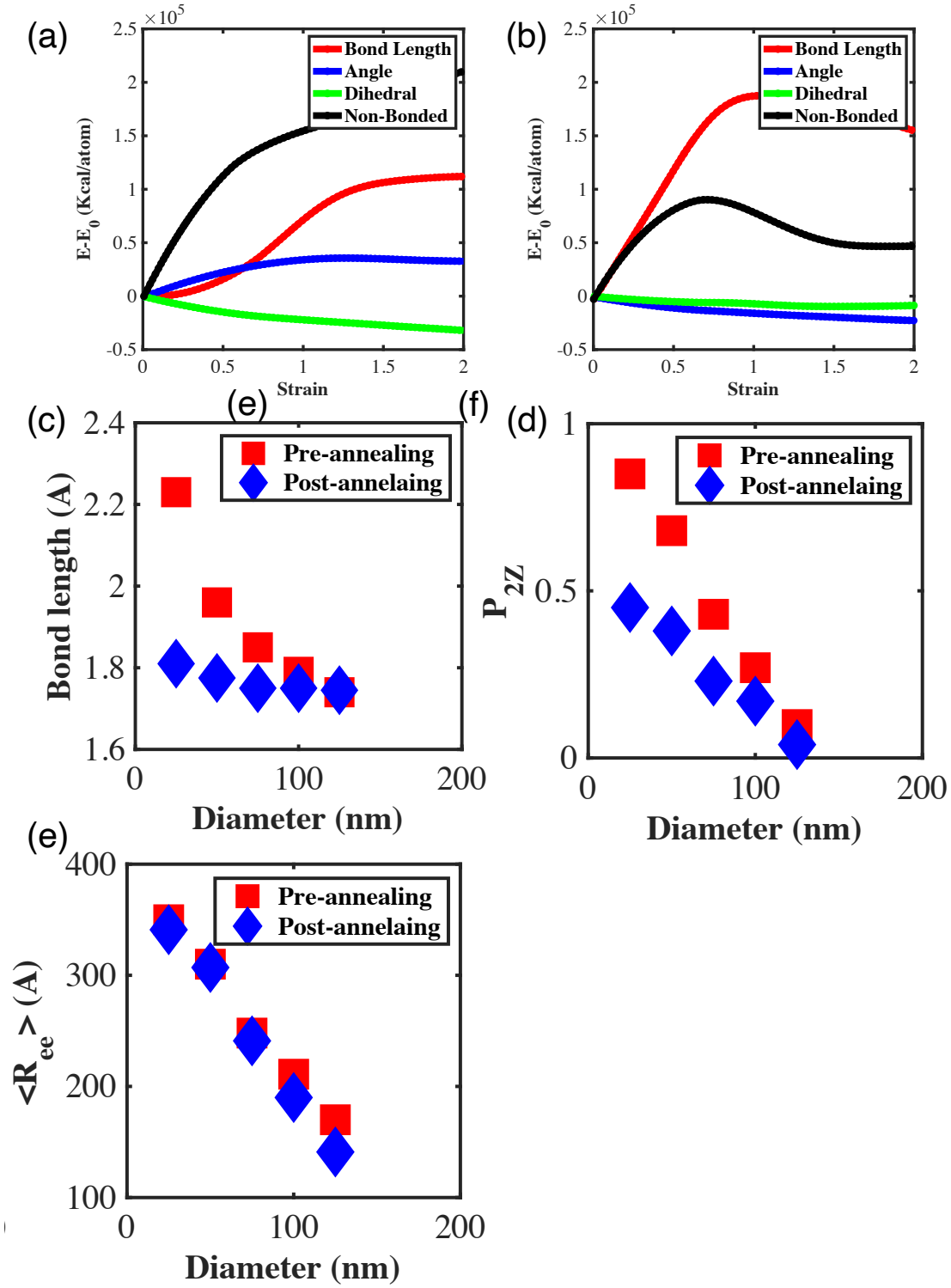

Figure S5 Evolution of the bond, angle, dihedral, and non-bonded energies during the tensile test for: (a) amorphous nanofiber, and (b) annealed nanofiber. Corresponding (c) bond length, (d) chain orientation parameter, and (e) backbone end-to-end distance extracted from the amorphous and the annealed nanofiber.

References

1. Vancoillie, S. et al. Parallelization of a multiconfigurational perturbation theory. J. Comput. Chem. **34**, 1937–1948 (2013).
2. Deng, S., Arinstein, A. & Zussman, E. Size-dependent mechanical properties of glassy polymer nanofibers via molecular dynamics simulations. J. Polym. Sci. Part B Polym. Phys. **55**, 506–514 (2017).
3. Hossain, D. et al. Molecular dynamics simulations of deformation mechanisms of amorphous polyethylene. Polymer (Guildf). **51**, 6071–6083 (2010).